Journal of the Serbian Chemical Society
JSCS@tmf.bg.ac.rs • www.shd.org.rs/JSCS
J. Serb. Chem. Soc. *84* (1) 27–40 (2019)
JSCS–5162
UDC 662.221+532.14:66.092:537.213:66.012.3
Original scientific paper

A simple relationship of bond dissociation energy and average charge separation to impact sensitivity for nitro explosives

ZHENG MEI[1], FENGQI ZHAO[2], SIYU XU[2] and XUEHAI JU[1]*

[1]*Key Laboratory of Soft Chemistry and Functional Materials of MOE, School of Chemical Engineering, Nanjing University of Science and Technology, Nanjing 210094, P. R. China and* [2]*Laboratory of Science and Technology on Combustion and Explosion, Xi'an Modern Chemistry Research Institute, Xi'an 710065, P. R. China*

(Received 4 April, revised 12 June, accepted 11 July 2018)

Abstract: The bond dissociation energy (*BDE*) of the weakest bonds in 33 explosives were calculated and analyzed using the B3LYP method with the 6-311++G** basis set. A comparison between *BDE* and the impact sensitivity H_{50} showed that cleavage of the weakest bond plays an important role in the initiation of detonation. Using the generalized gradient approximation (GGA) with the Perdew–Burke–Ernzerhof (PBE) method and dispersion-corrected density functional theory (DFT-D), the simulation of compressed TNT (2-methyl-1,3,5--trinitrobenzene) and royal demolition explosive (RDX, hexahydro--1,3,5-trinitro-1,3,5-triazine) crystals showed that an imbalance of the electrostatic surface potential (*ESP*) leads to molecular deformation and instability of the explosive under impact pressures. The average charge separation (*Π*) of the molecules was calculated and used to demonstrate the *ESP* balances. Based on the *BDE*, *Π* and the experimental H_{50} values, simple quantitative structure–sensitivity correlations were established for the nitro heterocycles, nitramines, picryl heterocycles and nitro aromatics, respectively. The fitting relationship is simple yet statistically significant with only two variables. The correlation coefficients, R^2, are larger than 0.8 with $F>F^{**}_{(0.05)}$ (95 % confidence intervals).

Keywords: electrostatic surface potential; nitro explosives; density functional theory; energetic compounds.

INTRODUCTION

Impact sensitivity is one of the most important characters of energetic materials, which determines the applying capabilities and regulatory policies for explosives, pyrotechnic compositions and propellants.[1] As an experimental quantity, impact sensitivity is commonly measured by a standard hammer fall from a testing height to a sample of the energetic material of a certain mass. The height

* Corresponding author. E-mail: xhju@njust.edu.cn
https://doi.org/10.2298/JSC180404059M

causing 50 % probability to initiate detonation is the measured quantity, which is denoted by H_{50}. Efforts to develop advanced energetic materials with both high detonation performance and low sensitivity have lasted for ages.[2–4] However, empirically, the impact sensitivity undesirably increases (or H_{50} decreases) as the detonation performance increases, while they are compatible for few explosives, such as 2,4-dinitroimidazole and 1,3,5-triamino-2,4,6-trinitrobenzene.[5] In order to lower the sensitivity, the contribution of the most crucial factors of the initiation should be quantified.

Due to the complexity of the realistic status and environment in energetic molecular crystals, impact-induced initiation involves complicated causes, *i.e.*, molecular, crystalline and physical factors.[6–8] According to the molecular factors, previous researchers proposed that the breaking of the weakest C–NO_2/N–NO_2 bonds in the molecules might be the key step in the initiation of detonation.[6,7] For example, the MP4 level calculation of Melius indicated that the N–NO_2 linkage is the first bond to break, which leads to a significant weakness of the second nearest neighbor bond in cyclotrimethylenetrinitramine (RDX) and cyclotetramethylenetetranitramine (HMX), thereby inducing complete decomposition of the molecules.[9] Rice *et al.* calculated the bond dissociation energies (*BDE*) of the bonds between the NO_2 groups and aromatic rings in some nitroaromatic molecules and established a positive qualitative relationship between *BDE* and H_{50}.[10] Moreover, Lienard and coworkers found that the *BDE* is related to the stability of drugs with respect to auto-oxidation.[11] Hence, the weakest bond strength as an important molecular factor of initiation is related to the impact sensitivity.

On the other hand, the molecular electrostatic surface potential (*ESP*) is another significant molecular factor that critically affects intermolecular interactions including electrostatic force, dispersion force and hydrogen bonding, all of which are related to the molecular crystalline properties. Thus, the *ESP* was also investigated as an important factor of initiation, which provided important predictive capabilities for some series of energetic materials. Politzer and Murray indicated that strong positive electrostatic potentials on the central portions of their molecular surfaces lead to the sensitivities of energetic compounds.[2] Meanwhile, their work also revealed that some crystalline factors, such as lattice free space and maximum heat of detonation per unit volume, influence the sensitivity. In another instance, Zhang *et al.* presented a correlation between the Mulliken charges of nitro group and the H_{50} value and provided capable prediction for several nitroaromatic compounds based on this correlation.[12]

The above efforts are truly remarkable successes that provided crucial intermolecular mechanisms and qualitative/quantitative correlations. However, correlations that involve not only local properties, such as the *BDE* of the weakest bond and the Mulliken charges of nitro groups, but also global properties, such as electrostatic imbalance of a molecular surface, are few. The more balanced the

ESP is, the smaller is the deviation of charge on the molecular surface. Much evidence shows that the *ESP* may correlate with impact sensitivity. Therefore, in order to clarify the different contributions of the molecular factors to the impact initiation for each type of nitro explosives, the *BDE* of the weakest bond and the imbalance of the molecular *ESP* as a whole were simultaneously considered and binary fittings to the experimental H_{50} of explosives of each type were performed. Based on the binary fittings, both the local feature (*BDE*) and the global property (electrostatic imbalance of a molecular surface) were involved, thus more predictable correlations could be established for the corresponding types of the explosives.

For this purpose, the *BDE* and the average *ESP* separation parameter Π for 11 nitro heterocycles, 7 nitramines, 9 picryl heterocycles, and 6 nitro aromatics, were calculated. These molecules consist of important and representative energetic materials. Specifically, the lattice electrostatic potential and crystalline structures for compressed 2,4,6-trinitrotoluene (TNT) and 1,3,5-trinitroperhydro-1,3,5-triazine (RDX) were demonstrated regarding different impact pressures, thereby revealing the relation between the *ESP* and the stability under various pressures. The fitting parameters for *BDE*, Π and H_{50} revealed the different contributions of the factors to impact-initiation, and provided predictive capabilities for the 4 types of nitro explosives. The relationship could aid future exploration of new advanced energetic materials with low impact sensitivities.

COMPUTATIONAL METHODS

Benchmark of the computational methods

Several methods of quantum chemistry were tested in this part, such as PM6, B3LYP, B3LYP with D3 dispersion correction (B3LYP-D3), B2PLYPD, and G4 method. The basis set for these methods was 6-311++g(d,p). In order to clarify the performances of these methods for the explosives, a reaction was designed to calculate the change of enthalpy:

$$CH_3NH_2 + CH_4 \xrightarrow{\Delta H} C_2H_6 + NH_3 \quad (1)$$

All the reactants and products are gaseous under standard conditions, and their experimental heats of formation were used to calculate the change in enthalpy and compare it with computational results. This reaction could be used to test the performance of the methods for computing the energies of bonds between C, N and H atoms. The computed total energy, total energy with zero-point energy, and enthalpy in standard conditions for the reactants and products are listed in Table I. The experimental heats of formation for CH_3NH_2, CH_4, C_2H_6 and NH_3 are –23.5, –74.6, –84.0 and –45.9 kJ mol^{-1}, respectively.[13-15] Using the heats of formation and the calculated energies, the change in enthalpies for reaction (1) are listed in Table II.

As could be seen in Table II, the G4 method provided excellent enthalpy changes compared with the experimental values. This is reasonable because the G4 method uses the 4-order Møller–Plesset perturbation theory (MP4) geometries and coupled cluster singles and doubles (CCSD) energies to obtain accurate bonding energies and vibrational modes. Meanwhile, the B3LYP, B3LYP-D3 and B2PLYPD methods provided enthalpy changes with small

deviations. Considering the accuracy and computational cost, the B3LYP method was selected to compute the explosives.

TABLE I. Computed total energy (*E*), total energy with zero-point energy (*E*+*ZPE*) and enthalpy in standard conditions (*H*) for CH_3NH_2, CH_4, C_2H_6 and NH_3

Compound	Method	*E* / a.u.	*E*+*ZPE* / a.u.	*H* / a.u.
CH_3NH_2	PM6	–0.0038	0.0533	0.0568
	B3LYP	–95.8939	–95.8301	–95.8267
	B3LYP-D3	–95.8982	–95.8344	–95.8310
	B2PLYPD	–95.7844	–95.7201	–95.7167
	G4	–95.7749	–95.7783	–95.7739
CH_4	PM6	–0.0196	0.0198	0.0227
	B3LYP	–40.5340	–40.4894	–40.4865
	B3LYP-D3	–40.5359	–40.4913	–40.4885
	B2PLYPD	–40.4743	–40.4294	–40.4266
	G4	–40.4624	–40.4653	–40.4615
C_2H_6	PM6	–0.0252	0.0419	0.0456
	B3LYP	–79.8566	–79.7823	–79.7788
	B3LYP-D3	–79.8620	–79.7877	–79.7842
	B2PLYPD	–79.7506	–79.6758	–79.6724
	G4	–79.7346	–79.7381	–79.7337
NH_3	PM6	–0.0050	0.0247	0.0276
	B3LYP	–56.5827	–56.5485	–56.5456
	B3LYP-D3	–56.5839	–56.5497	–56.5468
	B2PLYPD	–56.5204	–56.4858	–56.4829
	G4	–56.5147	–56.5176	–56.5138

TABLE II. The experimental and computed enthalpy changes for reaction (1)

Method	Δ*E* / a.u.	Δ(*E*+*ZPE*) / a.u.	Δ*H* / a.u.
Exp.	–	–	–31.69[a]
PM6	–17.76	–16.93	–16.69
B3LYP	–30.05	–29.43	–29.30
B3LYP-D3	–31.03	–30.41	–30.27
B2PLYPD	–32.36	–31.88	–31.72
G4	–31.69	–31.89	–31.69

[a]Experimental Δ*H* calculated from the heats of formation taken from the literature[13-15]

Bond dissociation energy

In order to obtain the *BDE* of the weakest bond in each of the energetic compounds, density functional theory (DFT) calculations using the B3LYP method with the 6-311++G** basis set were performed using the Gaussian 09 program package.[16] The DFT method, particularly the B3LYP functional and the 6-311G basis set not only provide reasonable structures of molecules and radicals containing CHNO elements, but they also provide accurate energies of the systems.[17-21] Thus, the computed energies, structures and populations could be used in the calculations of the *BDE* and *ESP* for the energetic compounds and the radicals. Considering the characteristics of the systems, polarization functions and diffusion functions were also involved.

The *BDE* of the R–NO_2 bond cleavage reaction $RNO_2 \rightarrow R + NO_2$ were calculated as follow:

$$BDE = E_R + E_{NO_2} - E_{RNO_2} \quad (2)$$

where E_R and E_{NO_2} are the energies of the two corresponding fragments, and E_{RNO_2} is the energy of the parent molecule. The dissociation is homolytic cleavage, so the spin multiplicity of the radicals is 2. Each energy term in (2) was computed following structural optimization and composed by the total energy and the zero-point vibrational energy *(ZPE*) for accuracy consideration.

Besides, the ring cleavage reaction involves only 1 biradical. Thus, the *BDE* was calculated by:

$$BDE = E_{rad} + E_{mol} \quad (3)$$

where E_{mol} and E_{rad} are the energies of the original molecule and the biradical from ring cleavage, respectively. In the *BDE* calculation of the furazan compounds in this work, the spin multiplicity of the biradical from ring cleavage is 1. The unrestricted functional was employed for the radicals and biradicals.

Electrostatic surface potential

As mentioned previously, the *ESP* is a crucial concept that influences intermolecular interactions and the crystal features of detonation initiation. Therefore, the *ESP* should be well characterized and accurately quantified to establish its correlation with impact sensitivity. Politzer *et al*. provided a successful quantification based on the positive and negative variances on the molecular surface.[22] According to the Politzer method, the electrostatic potential $V(r)$ created by the nuclei and electrons in the surrounding space of a molecule is given by:

$$V(r) = \sum_A \frac{Z_A}{|R_A - r|} - \int \frac{\rho(r')dr'}{|r' - r|} \quad (4)$$

where Z_A is the charge of nucleus A located at R_A and $\rho(r)$ is the electronic density. The $V(r)$ on an isosurface of an electronic density of 0.001 is the *ESP*, denoted as $V_S(r)$. The average of the *ESP* over the isosurface is given by:

$$\bar{V}_s = \frac{1}{n}\sum_{k=1}^{n} V_s(r_k) \quad (5)$$

Π is the average deviation of *ESP* over the surface:

$$\Pi = \frac{1}{n}\sum_{k=1}^{n} \left| V_s(r_k) - \bar{V}_s \right| \quad (6)$$

which is viewed as a balance characterization of *ESP*. A large Π indicates the electrostatic imbalance of a molecular surface, while a small Π implies the contrary.

By applying the space electrostatic potential distribution $V(r)$ calculated by Gaussian 09 program package[16] at the B3LYP/6-311++G** level, the average charge separation Π of the energetic compounds were obtained using Multiwfn 3.2 software developed by Lu and Chen.[23]

RESULTS AND DISCUSSION

BDE *of the weakest bonds*

In order to quantify the bond strength, the bond dissociation energies (*BDE*s) for the weakest bonds in 33 nitro energetic compounds were calculated and the results are presented in Table III. The experimental impact sensitivity H_{50} for the compounds were taken from the literature.[24–29]

TABLE III. The numbering, chemical name, molecular weight, experimental impact sensitivity, and calculated *BDE* for 33 nitro explosives

No.	Name	Formula	*MW* g mol^{-1}	Weakest bond	*BDE* kJ mol^{-1}	H_{50} cm
1	3-Nitro-1,2,4-triazole	$C_2H_2N_4O_2$	114.06	C–NO_2	265.02	320[a]
2	3-Nitro-1,2,4-triazol-5-one (NTO)	$C_2H_2N_4O_3$	130.06	C–NO_2	256.51	291[a]
3	4-Methyl-3,5-dinitro-4*H*-1,2,4-triazole	$C_3H_3N_5O_4$	173.09	C–NO_2	241.45	155[a]
4	5,5′-Dinitro-3,3′-bi-1*H*-1,2,4-triazole	$C_4H_2N_8O_4$	226.11	C–NO_2	261.01	153[a]
5	2,4,5-Trinitroimidazole	$C_3HN_5O_6$	203.07	C–NO_2	235.44	68[a]
6	2,4-Dinitroimidazole	$C_3H_2N_4O_4$	158.07	C–NO_2	259.87	100[a]
7	4,4′,5,5′-Tetranitro-2,2′-bi-1*H*-imidazole	$C_6H_2N_8O_8$	314.13	C–NO_2	239.66	37[a]
8	2,4,6-Trinitropyridine-1-oxide	$C_5H_2N_4O_7$	230.09	C–NO_2	230.45	20[a]
9	2,2′-(1,2-Diazenediyl)bis[3,5-dinitropyridine]	$C_{10}H_4N_8O_8$	364.19	C–NO_2	255.06	56[a]
10	3-Amino-4-nitrofurazan	$C_2H_2N_4O_3$	130.00	N–O	170.15	27[a]
11	4,4′-Dinitro-3,3′-bifurazan	$C_4N_6O_6$	228.00	N–O	165.05	13[a]
12	Cyc1otrimethylenetrinitramine (RDX)	$C_3H_6N_6O_6$	222.12	N–NO_2	141.96	24[a], 26[b]
13	Cyc1otetramethylenetetranitramine (HMX)	$C_4H_8N_8O_8$	296.16	N–NO_2	155.01	26[a], 29[b]
14	Hexanitrohexaazaisowurtzitane (CL-20)	$C_6H_6N_{12}O_{12}$	438.19	N–NO_2	132.32	17[c], 24[d]
15	Bis(trinitroethyl)nitramine	$C_4H_4N_8O_{14}$	388.12	N–NO_2	102.39	5[a]
16	1,3,3-Trinitroazetidine (TNAZ)	$C_3H_4N_4O_6$	192.09	N–NO_2	148.93	29[b]
17	*N*,*N*′-Dinitro-1-2-ethanediamine	$C_2H_6N_4O_4$	150.09	N–NO_2	172.89	34[a]
18	1,3,3,5,5-Pentanitropiperidine	$C_5H_6N_6O_{10}$	310.14	N–NO_2	139.55	14[a]
19	3-Picrylamino-1,2,4-triazole	$C_8H_5N_7O_6$	295.17	C–NO_2	214.28	320[a]
20	*N*-(2,4,6-trinitrophenyl)-1*H*-1,2,4-triazol-5-amine	$C_8H_6N_8O_6$	310.19	C–NO_2	215.09	230[a]
21	2-Nitro-1-picrylimidazole	$C_9H_4N_6O_8$	324.17	C–NO_2	252.39	312[a]
22	1-Picrylimidazole	$C_9H_5N_5O_6$	279.17	C–NO_2	223.06	314[a]
23	3,5-Dinitro-2,6-bis[2-(2,4,6-trinitrophenyl)--diazenyl]pyridine	$C_{17}H_5N_{13}O_{16}$	647.30	C–NO_2	222.01	33[a]
24	2,6-Bis(picrylamino)-3,5-dinitropyridine	$C_{17}H_7N_{11}O_{16}$	621.30	C–NO_2	211.76	63[a]
25	4-Nitro-*N*-(2,4-trinitrophenyl)--1,2,5-oxadiazol-3-amine	$C_8H_3N_7O_9$	341.00	N–O	165.69	60[a]
26	N^3-(2,4,6-trinitrophenyl)--1,2,5-oxadiazol-3,4-diamine	$C_8H_5N_7O_7$	311.00	N–O	173.88	120[a]
27	N^3,N^4-Bis(2,4,6-trinitrophenyl)--1,2,5-oxadiazol-3,4-diamine	$C_{14}H_6N_{10}O_{13}$	522.00	N–O	175.15	71[a]
28	2,4,6-Trinitrophenylmethylnitroamine (Tetryl)	$C_7H_5N_5O_8$	287.14	N–NO_2	104.28	32[a]

TABLE III. Continued

No.	Name	Formula	*MW* g mol^{-1}	Weakest bond	*BDE* kJ mol^{-1}	H_{50} cm
29	1,3,5-Trinitrobenzene (TNB)	$C_6H_3N_3O_6$	213.10	C–NO_2	255.05	100[a]
30	1,3,5-Triamino-2,4,6-trinitrobenzene (TATB)	$C_6H_6N_6O_6$	258.15	C–NO_2	269.90	490[a]
31	1,3-Diamino-2,4,6-trinitrobenzene (DATB)	$C_6H_5N_5O_6$	243.13	C–NO_2	274.58	320[a]
32	2,4,6-Trinitrotoluene (TNT)	$C_7H_5N_3O_6$	227.13	C–NO_2	235.28	160[a]
33	2,4,6-Trinitroaniline	$C_6H_4N_4O_6$	228.12	C–NO_2	259.66	177[a]

[a,b,c,d]Experimental data taken from references 24, 25–27, 28 and 29, respectively

In Table III, compounds **1**–**11** are nitro heterocycles, **12**–**18** are nitramines, **19**–**27** are picryl heterocycles, and **28**–**33** are nitro aromatics.

The weakest bonds are the C–NO_2 single bonds, the N–NO_2 single bonds, and the N–O single bonds in the furazan rings, corresponding to the different compounds. The *BDE* of the weakest C–NO_2 bonds are in the range of 210 to 280 kJ mol^{-1}, which are larger than those of the weakest N–NO_2 bonds (100–180 kJ mol^{-1}) and the weakest N–O bonds (160–180 kJ mol^{-1}) in the furazan rings. It is noted that bis(trinitroethyl)nitramine (**15**) with the lowest H_{50} (5 cm) corresponded to the smallest *BDE* (102.39 kJ mol^{-1}), while TATB with the highest H_{50} (490 cm) corresponded to the second largest *BDE* (269.90 kJ mol^{-1}).

The *BDE* and the H_{50} for all the 33 energetic compounds are demonstrated in Fig. 1. It could be seen that H_{50} are smaller as *BDE* are smaller. However, some H_{50} values significantly increase when the *BDE* exceed 170 kJ mol^{-1}. This indicated that, as a whole, the *BDE* and the H_{50} are positively related.

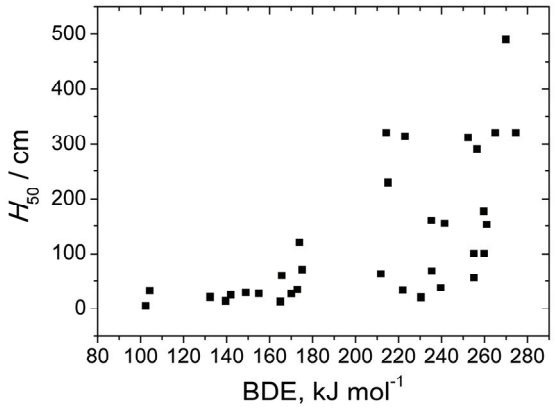

Fig. 1. *BDE* values and the corresponding H_{50} for all the energetic compounds.

Nevertheless, this relation was not sufficient to establish a predicable correlation for the different type of nitro explosives. Thus, the *ESP* factors were introduced in the following section.

Average charge separation of ESP

The molecular *ESP* could be employed to represent intermolecular factors for the initiation of detonation. In order to reveal the effect of ESP on the impact sensitivity, two representative explosives were specifically investigated under different pressures. The distribution of the electrostatic potential of TNT and RDX crystals under pressures of 0, 5 and 10 GPa were calculated using the Material Studio 6.0 package with CASTEP and DMol3 modules by the GGA-PBE method, including the norm conserving pseudopotential and the Grimme DFT-D dispersion correction.[30–34] The initial crystalline structures of TNT[35] and RDX[36] were taken from the literature and the computational results are shown in Fig. 2a and b, respectively. It could be seen that the negative charge in the space between the molecules shrunk with increasing pressure, resulting in changes in the charge distributions. The change of the electrostatic potential for TNT was larger than that for RDX, which may have been caused by the *ESP* of TNT being more balanced than that of RDX and thus being compressed more easily.

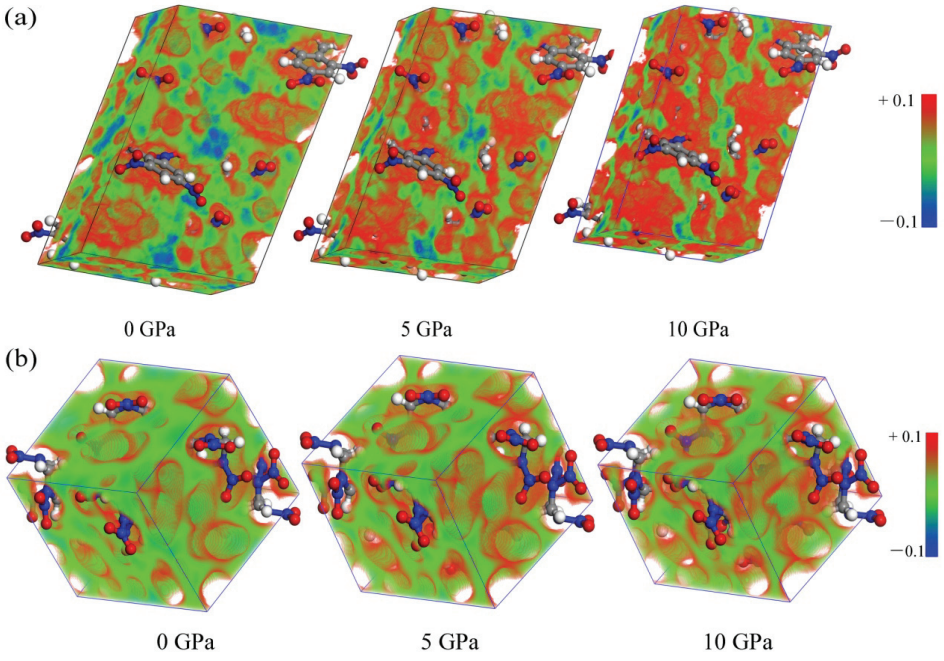

Fig. 2. The electrostatic potential distribution of TNT (a) and RDX (b) crystals under 0, 5 and 10 GPa.

To verify this speculation, the lattice parameters a, b, c and the ratio of compression, R_p, for the TNT and RDX crystal under the different pressures are listed in Table IV. In order to demonstrate the deformation of the molecules under pres-

sure, the average NO_2–ring dihedral angle φ_{ave} and the dihedral angle changing $\Delta\varphi_{ave}$ of the TNT and RDX molecules in the gas and condensed phase under different pressures were listed in Table IV. The average charge separation Π for isolated TNT and RDX molecules are also given in Table IV.

TABLE IV. The lattice parameters *a*, *b*, *c* as well as the compression ratio R_p, the average NO_2–ring dihedral angle φ_{ave} and the change in the dihedral angle $\Delta\varphi_{ave}$ of the TNT and RDX molecules in gas and condensed phase under different pressures, and the average charge separation Π on the ESP of isolated TNT and RDX molecules

Cmpd.	Phase	*a* / Å	*b* / Å	*c* / Å	R_p / %	φ_{ave} / °	$\Delta\varphi_{ave}$ / °	Π / kJ mol^{-1}
TNT	gas	–	–	–	–	0.20	–	64.02
	0 GPa	15.0669	6.0608	20.9885	–	0.34	0.14	–
	5 GPa	14.4354	5.6735	19.3489	17.32	1.62	1.42	–
	10 GPa	14.0656	5.5125	18.7446	24.17	2.22	2.02	–
RDX	gas	–	–	–	–	23.51	–	72.97
	0 GPa	11.4883	10.7584	13.3479	–	19.61	– 3.91	–
	5 GPa	10.8442	10.0061	12.7497	16.14	19.41	– 4.10	–
	10 GPa	10.4890	9.6419	12.5122	23.30	18.51	– 5.00	–

In Table IV, the average charge separation Π of TNT is smaller than that of RDX, but the compression ratio R_p of TNT is larger than that of RDX for all applied pressures. This implies that the *ESP* of TNT is more balanced and the intermolecular electron cloud in the TNT crystal is more easily compressed. In addition, the *ESP* of RDX is less balanced, leading to difficulty in its compression. Furthermore, the $\Delta\varphi_{ave}$ of RDX were significantly larger than those of TNT, indicating that the compression of RDX crystals requires more intensive deformation of the molecules, resulting in instability of the explosive. Based on the above analysis, it could be concluded that the intermolecular electron cloud plays a role as a buffer during impact. Under the impact pressures, the 'buffer' would be soft and protect the molecules when the *ESP* was balanced, or it would become stiff and lead to deformation of the molecules when the *ESP* was imbalanced. In this view, Π was negatively correlated to H_{50}.

The above analysis for compressed TNT and RDX crystals reveals that the average charge separation Π of the *ESP* is an important factor for the compression response for molecular crystals. In order to establish a correlation between the crystal factor and the impact sensitivities, the Π of isolated molecules were calculated and are listed in Table V. It is noteworthy that the insensitive explosive TATB with the smallest Π corresponded to the largest H_{50} (490 cm).

Correlations of BDE *and* Π *to impact-sensitivities for the 4 types of nitro explosives*

As discussed above, the *BDE* is positively correlated with the H_{50}, while the Π is negatively correlated to the H_{50}. Based on this principle, a simple fitting formula was designed with a combination of *BDE* and Π:

$$H_{50} = a + b\frac{BDE}{MW} + c\frac{MW}{\Pi} \quad (7)$$

where a, b and c are fitting coefficients, MW / g mol^{-1} is the molar mass, BDE / kJ mol^{-1} is the bond dissociation energy of the weakest bond and Π / kJ mol^{-1} is the average charge separation of the *ESP*.

TABLE V. The type, numbering, chemical name, average charge separation of the *ESP* and impact sensitivities of the energetic molecules

Type	Cmpd.	Π / kJ mol^{-1}	H_{50} / cm
Nitro heterocycles	**1**	99.79	320[a]
	2	80.67	291[a]
	3	79.45	155[a]
	4	76.90	153[a]
	5	74.64	68[a]
	6	142.26	100[a]
	7	78.78	37[a]
	8	72.72	20[a]
	9	65.14	56[a]
	10	67.74	27[a]
	11	49.29	13[a]
Nitramines	**12**	72.97	24[a], 26[b]
	13	81.25	26[a], 29[b]
	14	68.53	17[c], 24[d]
	15	135.69	5[a]
	16	119.41	29[b]
	17	88.78	34[a]
	18	133.60	14[a]
Picryl heterocycles	**19**	69.16	320[a]
	20	71.17	230[a]
	21	69.71	312[a]
	22	66.69	314[a]
	23	64.68	33[a]
	24	65.61	63[a]
	25	63.55	60[a]
	26	69.20	120[a]
	27	69.75	71[a]
Nitro aromatics	**28**	68.32	32[a]
	29	67.36	100[a]
	30	61.80	490[a]
	31	66.23	320[a]
	32	64.02	160[a]
	33	68.45	177[a]

[a,b,c,d]Experimental data taken from the References 24, 25–27, 28 and 29, respectively

The fittings were performed according to 4 types of the energetic compounds, including nitro heterocycles, nitramines, picryl heterocycles and nitro

aromatics. For the compounds with different experimental H_{50} from different references, the averaged H_{50} were employed in the fitting. The fitting equations are in Table VI.

TABLE VI. The fitting equation, number of used data points N_p, R^2, variance test parameter F and $F^{**}_{(0.05)}$, and the significance level for H_{50} for the 4 types of nitro explosives

Type	Fitting equation	N_p	R^2	F	$F^{**}_{(0.05)}$	Sig.
Nitro heterocycles	$H_{50} = -424.7 + 304.7\int \frac{BDE}{MW} + 51.69\frac{MW}{\Pi}$	11	0.878	28.72	4.459	0.000
Nitramines	$H_{50} = -8.705 + 36.50\frac{BDE}{MW} + 3.065\frac{MW}{\Pi}$	7	0.827	9.585	6.944	0.030
Picryl heterocycles	$H_{50} = -358.2 + 768.9\frac{BDE}{MW} + 15.75\frac{MW}{\Pi}$	9	0.926	37.58	4.737	0.000
Nitro aromatics	$H_{50} = -2246 + 698.7\frac{BDE}{MW} + 480.9\frac{MW}{\Pi}$	6	0.990	137.8	9.552	0.001

The fitting coefficients b and c are both positive numbers, which is verification of the postulation discussed above. All the correlation coefficients R^2 were larger than 0.8, especially, those of the nitro aromatics are 0.990.

All the F values for the fittings are larger than the corresponding $F^{**}_{(0.05)}$ value, indicating that the linear relationships are significant in the confidence interval of 95 %. These indicate that the fitting equations are reasonable to provide reliable contributions of the factors.

The fitting coefficients b and c in the equations show that the ratio of contributions for *BDE* and Π factors are about 6/1, 12/1, 49/1 and 1.5/1 for the nitro heterocycles, nitramines, picryl heterocycles and nitro aromatics, respectively. The contribution of Π was similar to the *BDE* for the nitro aromatics, implying the role of the *ESP* is as important as the *BDE* in the impact initiation for the nitro aromatics. Besides, the contribution of the *BDE* factor is much larger than that of the Π factor for picryl heterocycles. Based on the equations, the comparisons of the predicted H_{50} and experimental H_{50} for the 4 types of energetic compounds are shown in Fig. 3.

The points are close to the fitting lines and showed good consistency, especially for the nitro aromatics.

CONCLUSIONS

First, the *BDE* of the weakest bonds for 33 nitro explosives were calculated at the DFT/B3LYP/6-311++G** level and were compared with the experimental impact sensitivities. The results showed that the *BDE* and H_{50} were roughly positively correlated.

Secondly, using the GGA approximation with the PBE method, the norm conserving pseudopotential and DFT-D correction, the simulation of compressed TNT

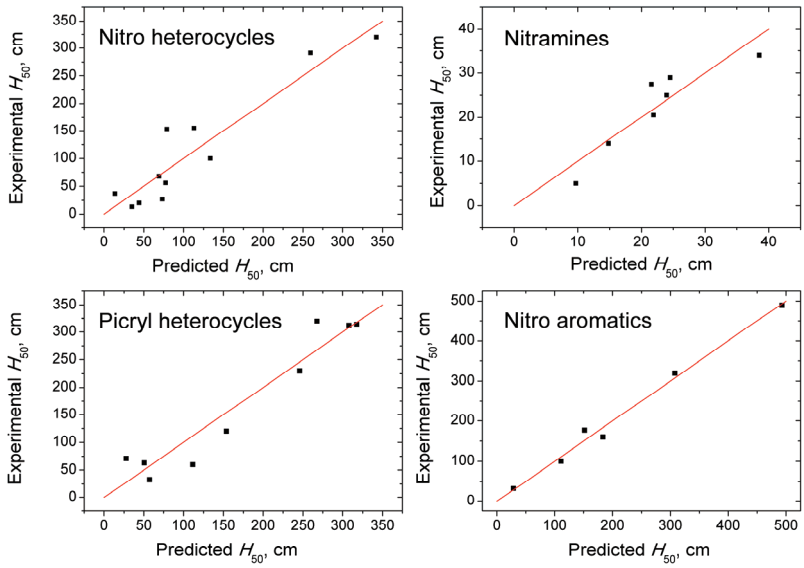

Fig. 3. Relationships of experimental and predicted H_{50} for the four types of nitro compounds.

and RDX crystals revealed the influence of the *ESP* on the H_{50}. It was observed that the TNT molecule is more in electrostatic balance than RDX molecule, indicating that TNT is more easily compressed. However, the compression of an RDX crystal leads to more intensive deformation of the molecules, which results in the instability of RDX under impact pressure. The analysis showed that the average charge separation *Π* is negatively correlated to the H_{50}.

Based on the *BDE*, *Π* and experimental H_{50}, structure–sensitivity correlations for the 4 types of energetic compounds were established. Statistical analysis showed that the linear relationships are significant. The predicted H_{50} values were in good agreement with the experimental H_{50} value. The fitting equations reveal the contributions of the *BDE* and *ESP* factors regarding impact initiation of detonation.

Acknowledgement. Z. Mei thanks the Innovation Project for Postgraduates in Universities of Jiangsu Province.

ИЗВОД

ПРОСТ ОДНОС ЕНЕРГИЈЕ ДИСОЦИЈАЦИЈЕ ВЕЗЕ И ПРОСЕЧНОГ РАЗДВАЈАЊА НАЕЛЕКТРИСАЊА СА ОСЕТЉИВОШЋУ НА УДАР КОД НИТРО ЕКСПЛОЗИВА

ZHENG MEI[1], FENGQI ZHAO[2], SIYU XU[2] и XUEHAI JU[1]

[1]*Key Laboratory of Soft Chemistry and Functional Materials of MOE, School of Chemical Engineering, Nanjing University of Science and Technology, Nanjing 210094, P. R. China и* [1]*Laboratory of Science and Technology on Combustion and Explosion, Xi'an Modern Chemistry Research Institute, Xi'an 710065, P. R. China*

Енергије дисоцијације везе (*BDE*) најслабијих веза код 33 експлозива израчунате су и анализиране користећи B3LYP метод са 6-311++G** базичним скупом. Поређење *BDE*

и осетљивости на удар H_{50} показује да раскидање најслабије везе игра значајну улогу у иницирању детонације. Коришћење GGA апроксимације са PBE методом и DFT-D поправком, симулација сабијених TNT и RDX кристала показује да неравнотежа површине електростатичког потенцијала (*ESP*) доводи до деформације молекула и до нестабилности експлозива при ударним притисцима. Просечно раздвајање наелектрисања (Π) у молекулима је израчунато и употребљено да се прикажу *ESP* баланси. На основу *BDE*, Π и експерименталних H_{50}, утврђене су просте квантитативне корелације структуре и осетљивости за нитро хетероцикле, нитрамине, пикрил хетероцикле односно нитро аромате. Релација фитовања је једноставна а ипак статистички значајна и са само две промењљиве. Коефицијенти корелације R^2 су већи од 0,8 са $F>F^{**}_{(0,05)}$ (95 % интервалом поузданости).

(Примљено 4. априла, ревидирано 12. јуна, прихваћено 11. јула 2018)

REFERENCES

1. National Research Council, *Advance Energetic Materials*, The National Academies Press, Washington DC, 2004 (https://www.nap.edu/catalog/10918/advanced-energetic-materials)
2. P. Politzer, J. S. Murray, *J. Mol. Model.* **21** (2015) 2578 (http://dx.doi.org/10.1007/s00894-015-2578-4)
3. P. Politzer, J. S. Murray, *Propellants, Explo. Pyrotech.* **41** (2016) 414 (http://dx.doi.org/10.1002/prep.201500349)
4. J. Li, *J. Phys. Chem. B* **114** (2010) 2198 (http://dx.doi.org/10.1021/jp909404f)
5. J. J. Sabatini, K. D. Oyler, *Crystals* **6** (2016) 5 (http://dx.doi.org/10.3390/cryst6010005)
6. M. H. Keshavarz, M. Ghaffarzadeh, M. R. Omidkhah, K. Farhadi, *Z. Anorg. Allg. Chem.* **24** (2017) 2158 (http://dx.doi.org/10.1002/zaac.201700400)
7. C. Y. Zhi, X. L. Cheng, *Propellants, Explo. Pyrotech.* **35** (2010) 555 (http://dx.doi.org/10.1002/prep.200900092)
8. T. B. Brill, K. J. James, *Chem. Rev.* **93** (1993) 2667 (http://dx.doi.org/10.1021/cr00024a005)
9. C. F. Melius, *J. Phys. Colloq.* **48** (1987) 341 (https://doi.org/10.1051/jphyscol:1987425)
10. B. M. Rice, S. Sahu, F. J. Owens, *J. Mol. Struct.: THEOCHEM* **583** (2002) 69 (https://doi.org/10.1016/S0166-1280(01)00782-5)
11. P. Lienard, J. Gavartin, G. Boccardi, M. Meunier, *Pharm. Res.* **32** (2015) 300 (https://doi.org/10.1007/s11095-014-1463-7)
12. C. Y. Zhang, Y. J. Shu, Y. G. Huang, *J. Energ. Mater.* **2** (2005) 107 (https://doi.org/10.1080/07370650590936433)
13. J. G. Aston, C. W. Siller, G. H. Messerly, *J. Am. Chem. Soc.* **59** (1937) 1743 (https://doi.org/10.1021/ja01288a054)
14. J. A. Manion, *J. Phys. Chem. Ref. Data* **31** (2002) 123 (https://doi.org/10.1063/1.1420703)
15. M. W. Chase, *J. Phys. Chem. Ref. Data*, *Monogr.* **9** (1998) 1 (https://web-book.nist.gov/cgi/cbook.cgi?ID=C7664417&Units=SI&Mask=1#Thermo-Gas)
16. *Gaussian 09, Revision E.01*, Gaussian, Inc., Wallingford CT, 2009 (http://gaussian.com/g09citation/)
17. S. Y. Mary, E. S. Al-Abdullah, H. I. Aljohar, B. Narayana, P. S. Nayak, B. K. Sarojini, S. Armakovic, S. J. Armakovic, C. Van Alsenoy, A. A. El-Emam, *J. Serb. Chem. Soc.* **83** (2018) 1 (https://doi.org/10.2298/JSC170103056M)

18. F. Vlahovic, S. Ivanovic, M. Zlatar, M. Gruden, *J. Serb. Chem. Soc.* **82** (2017) 1369 (https://doi.org/10.2298/JSC170725104V)
19. X. H. Li, R. Z. Zhang, X. Z. Zhang, *J. Hazard. Mat.* **183** (2010) 622 (https://doi.org/10.1016/j.jhazmat.2010.07.070)
20. X. H. Li, Z. X. Tang, X. D. Yang, *Int. J. Quantum Chem.* **109** (2009) 1403 (https://doi.org/10.1002/qua.21952)
21. X. J. Xu, H. M. Xiao, X. H. Ju, *J. Phys. Chem., A* **110** (2006) 5929 (https://doi.org/10.1021/jp0575557)
22. P. Politzer, J. S. Murray, *Struct. Chem.* **28** (2017) 1045 (https://doi.org/10.1007/s11224-016-0909-4)
23. T. Lu, F. W. Chen, *J. Mol. Graphics Modell.* **38** (2012) 314 (https://doi.org/10.1016/j.jmgm.2012.07.004)
24. *Chemistry and Physics of Energetic Materials*, S. N. Bulusu, Ed., Springer Science & Business Media, New York, 2012 (https://www.springer.com/us/book/9780792307457)
25. P. F. Pagoria, G. S. Lee, A. R. Mitchell, *Thermochim. Acta* **384** (2002) 187 (https://doi.org/10.1016/S0040-6031(01)00805-X)
26. A. V. Dubovik, A. V. Apolenis, V. E. Annikov, E. I. Aleshkina, *Combust., Explos. Shock Waves* **44** (2008) 360 (https://doi.org/10.1007/s10573-008-0044-7)
27. R. D. Gilardi, R. J. Butcher, *Acta Crystallogr., E* **57** (2001) 757 (https://doi.org/10.1107/S1600536801011722)
28. R. L. Simpson, P. A. Urtiew, D. L. Ornellas, *Propellants, Explo. Pyrotech.* **22** (1997) 249 (https://doi.org/10.1002/prep.19970220502)
29. R. Sivabalan, G. M. Gore, U. R. Nair, *J. Hazard. Mat.* **139** (2007) 199 (https://doi.org/10.1016/j.jhazmat.2006.06.027)
30. *Discovery Studio Modelling Environment*, Accelrys Software Inc., Release 6.0, San Diego, CA, 2007
31. S. J. Clark, M. D. Segall, C. J. Pickard, P. J. Hasnip, M. I. Probert, K. Refson, M. C. Payne, *Z. Kristallogr. – Cryst Mater.* **220** (2005) 567 (https://doi.org/10.1524/zkri.220.5.567.65075)
32. B. Delley, *J. Chem. Phys.* **92** (1990) 508 (https://doi.org/10.1063/1.458452)
33. J. P. Perdew, K. Burke, M. Ernzerhof, *Phys. Rev. Lett.* **77** (1996) 3865 (https://doi.org/10.1103/PhysRevLett.77.3865)
34. S. Grimme, J. Antony, S. Ehrlich, H. Krieg, *J. Chem. Phys.* **132** (2010) 154104 (https://doi.org/10.1063/1.3382344)
35. R. M. Vrcelj, J. N. Sherwood, A. R. Kennedy, H. G. Gallagher, T. Gelbrich, *Cryst. Growth Des.* **3** (2003) 1027 (https://doi.org/10.1021/cg0340704)
36. V. V. Zhurov, E. A. Zhurova, A. I. Stash, A. A. Pinkerton, *Acta Crystallogr., A* **67** (2011) 160 (https://doi.org/10.1107/S0108767310052219).